Peer-reviewed version available at *Molecules* **2018**, *23*, 1411; doi:10.3390/molecules23061411

Polyphenols from *Tamarix nilotica*: LC–ESI-MS^n Profiling and *in-vivo* Antifibrotic Activity

Ahmed Sekkien[1], Noha Swilam[1]*, Shrief Ebada[2], Ahmed Esmat[3], Ahmed H. El-Khatib[4,5], Michael W. Linscheid[5], Abdel Nasser Singab[2]

Affiliation

[1] Department of Pharmacognosy, Faculty of Pharmacy, British University in Egypt (BUE), Cairo 11837, Egypt
[2] Department of Pharmacognosy, Faculty of Pharmacy, Ain Shams University, Cairo 11566, Egypt
[3] Department of Pharmacology and Toxicology, Faculty of Pharmacy, Ain Shams University, Cairo 11566, Egypt
[4] Department of Pharmaceutical Analytical Chemistry, Faculty of Pharmacy, Ain Shams University, Cairo 11566, Egypt
[5] Laboratory of Applied Analytical and Environmental Chemistry, Department of Chemistry, Humboldt-Universität zu Berlin, Berlin, Germany

*** Correspondence**

Dr. Noha Swilam, Department of Pharmacognosy, Faculty of Pharmacy, British University in Egypt (BUE), El Sherouk City, Cairo, Greater Cairo 11837-P.O. Box 43, Egypt; Noha.Swilam@bue.edu.eg, Phone: +201091011139, Fax: +20226300013

ABSTRACT

Tamarix nilotica (Ehrenb.) Bunge (Tamaricaceae), an indigenous plant to the Middle East region, is well-known as a medicinal plant for treating many human ailments. The current study aimed at exploring the polyphenols profile of *T.nilotica* alcohol soluble fraction of aqueous extract, assessing its *in-vivo* antifibrotic activity and the possible underlying mechanism, to unravel the impact of quantitative difference of sulphated polyphenols content on the antifibrotic activity of *T.nilotca* grown in two different habitats. Polyphenols profiling of *T. nilotica* extracts was performed using HPLC-HRESI-QTOF-MS-MS. The major polyphenol components included sulphated flavonoids, phenolic acids and free aglycones. The antifibrotic activity was evaluated through carbon tetrachloride-induced liver fibrosis in rats. Biochemical evaluations revealed that both fractions ameliorated the increased levels of hepatic aminotransferases, lipid peroxidation, hydroxyproline, α-smooth muscle actin (*α*-SMA), tumor necrosis factor-*α* (TNF-*α*), cyclooxygenase-2 (COX-2) and nuclear factor kappa B (NF-κB). Moreover, both fractions reduced catalase activity (CAT) and enhanced hepatic glutathione (GSH) content. Histopathological imaging undoubtedly confirmed such results. In conclusion, *T. nilotica* polyphenols rich fraction exhibited potential antifibrotic activity in rats. Significant alterations in GSH levels were recorded based on sulphated polyphenol metabolites content.

Keywords: *Tamarix nilotica*; Tamaricaceae; polyphenols; HPLC/HRESI/MS/MS; antifibrotic activity.

Peer-reviewed version available at Molecules 2018, 23, 1411; doi:10.3390/molecules23061411

1. Introduction

Hepatic fibrosis is a consequence of chronic liver diseases such as chronic hepatitis C virus (HCV) infection, alcohol abuse and non-alcoholic steatohepatitis (NASH) [1]. Hepatic fibrosis is characterized by an excessive accumulation of extracellular matrix (ECM) proteins including collagen as a common wound healing response distorting the normal hepatocellular architecture and forming a fibrous scar, which subsequently develops into hepatocellular nodules or an irreversible complication known as liver cirrhosis [2]. In the developing and the developed countries, liver cirrhosis represents an end-stage liver complication where liver transplantation becomes the only treatment choice, which is even not easy to achieve with regards to the number of donor organs available and the clinical condition of the potential recipients [3].

Therefore, research interests have been directed toward hepatic fibrosis several decades ago as the last reversible phase of complicated chronic hepatic diseases before turning into liver cirrhosis [1]. Based on the inconsistent effectiveness of treatment protocols using corticosteroids and interferon in chronic liver diseases and their complications, much attention have been drawn to herbal remedies as a last resort to help regenerating hepatocytes in liver fibrosis [4]. This notion was practically proven by the sudden rise in the popularity and use of herbal drugs by liver patients (up to 65%) within few years due to the fact that herbal remedies

represent undoubtedly an easily accessible, affordable and safe alternative to the current treatment protocols which turned out to be explicitly inadequate [4].

Genus *Tamarix* is native to Africa as well as Eurasian region, the genus comprises over 50 species including *T. nilotica* which is an evergreen trees or shrubs that can grow up to 5 m [5]. *Tamarix nilotica* have been widely incorporated in folk medicine of many societies and cultures for the treatment of sores, wounds, spleen oedema or uterus infections, while the extract itself has been used as an antiseptic [6] [7].

Former scientific reports proved that *T. nilotica* flowers possesses *in-vivo* hepatoprotective properties [8] which inspired this study to compare the antifibrotic activity of alcohol soluble fraction of aqueous extract of *T. nilotica* aerial parts from two different habitats, Egypt (ETN) and Saudi Arabia (STN) and their secondary metabolites profiling using HPLC/HRESI/MS/MS.

2. Results

2.1. Polyphenols Metabolic profiling

Chemical investigation of alcohol soluble fraction of aqueous extract of ETN and STN was conducted via HPLC/HRESI/MS/MS and dereplication tools using the natural product databases and comparison with the reported literature. Results (Tables 1 and 2) revealed that both fractions feature the abundance of polyphenol

secondary metabolites including flavonoid glycosides, methylated flavonoid aglycones, phenylpropanoids together with different sulphated compounds.

The negative ion mode profile of ETN showed three major peaks corresponding to methyl ferulate – sulphate, ferulic acid - sulphate derivative and coniferyl alcohol sulphate derivative. Peak of [M-H] - at m/z 287 and a fragment ion at m/z 207 comparable to removal of (SO3) group were in consistence with those reported for methyl ferulate -3-O-sulphate [9]. Isoferulic acid 3-*O*-sulphate was identified with $[M-H]^-$ at m/z 273 and a base peak signal at m/z 193 standing for the deprotonated phenolic acid [10]. Coniferyl alcohol 4-*O*-sulphat showed $[M-H]^-$ peak at m/z 259 and a fragment ion at m/z 179 after the loss of (SO_3) group [11]. The chromatogram further showed a molecular ion peak at m/z 299 along with fragment ion at m/z 284 as a result of losing a (CH_3) group assigned for Kaempferide [9]. Gallic acid was identified after showing a peak at m/z 169 and a fragment at m/z 125 as described by [12] [13]. A molecular ion peak at m/z 483 with fragment ion at m/z 313 due to loss of galloyl moiety proved the existence of nilocitin [14]. Kaempferol 7,4' dimethyl ether 3- *O*-sulphate was identified by a peak at m/z 393 and a fragment ion at m/z 313 indicating desulphonation [15]. A peak of the deprotonated ion at m/z 315 accompanied by a fragment ion at m/z 300 due to demethylation were similar to those reported for tamarixetin [16] [9] [17]. Kaempferol showed a molecular ion peak at m/z 285 [18] [15]. Another peak at m/z 193 corresponding to

deprotonated isoferulic acid showing a base peak at m/z 178 after the loss of a methyl group was detected [19] [17]. Quercetin was identified by a molecular ion peak at m/z 301 [18] [15]. Furthermore, a peak of [M-H]- m/z 197 representing methyl gallate 4-methyl ether showing fragments at m/z 182 and 167 indicating successive demethylation [18] [15]. Another peak appeared at m/z 461 referring to Kaempferol 3-*O*-β-glucronide with a daughter ion fragment at m/z 285 that belongs to the deprotonated free aglycone [15]. Further examination revealed the presence of 4'-*O*-methyl quercetin 3-*O*- β -hexoside at $[M-H]^-$ m/z 477 and a base peak at m/z 315 due to cleavage of the *O*-glycosidic bond release of the free aglycone and loss of the sugar moiety and another fragment at m/z 300 representing demethylation [16]. Kaempferol 4'-methyl ether 3-*O*-Sulphate was characterized by a molecular ion peak at m/z 379, the removal of (SO_3) moiety was responsible for the base peak at m/z 299 [11]. Finally, tamarixetin 3-*O*-sulphate was identified at m/z 395 and a base peak at m/z 315 standing for the loss of (SO_3) group [11] [17]. *n*-feruloyltyramine was only detected through inspection of the positive ion mode showing a major peak of $[M+H]^+$ at m/z 314 and a fragment at m/z 177 that represents the loss of ferulic aldehyde [20] [21].

Quantitative difference in polyphenols profile of ETN and STN was proved, whereas kaempferol 4'-methyl ether 3-*O*-sulphate, methyl ferulate-3-*O*-sulphate,

Peer-reviewed version available at Molecules 2018, 23, 1411; doi:10.3390/molecules23061411

123 isoferulic acid-3-*O*-sulphate and tamarixetin 3-sulphate were the major
124 polyphenols of STN extract.

125 *2.2. Total phenolic content*

126 The total phenolic contents of ETN and STN were determined through a
127 calibration curve using gallic acid as a standard. Results (Table 3) are presented in
128 equivalent milligrams of gallic acid per 1.0 g of dried extract and they revealed that
129 STN possesses a relatively higher total phenolic content (111.8 mg GA/g extract)
130 compared to ETN (95.1 mg GA/g extract).

131 *2.3. Oxygen radical absorbance capacity (ORAC assay)*

132 The antioxidant activities of ETN and STN were tested by the ORAC assay using
133 Trolox as a positive control. Both extracts exhibited a pronounced antioxidant
134 activity with ED_{50} values of 6.38 and 9.32 µg/mL, respectively, which are
135 significantly lower than that of the reference standard Trolox (ED_{50} = 27.0 µg/mL),
136 (Fig.1).

137 *2.4. Hepatotoxicity indices*

138 The exposure to CCl_4 caused a significant escalation in the levels of serum AST
139 and ALT levels by 3 folds when compared to the control group. Co-administration
140 of silymarin with CCl_4 significantly lowered the AST and ALT levels near to the
141 normal levels. Moreover, the concurrent administration of ETN with CCl_4 caused a
142 dose related decrease in the levels of the AST and ALT by 61% and 60%

143 respectively as compared to the CCl_4 intoxicated group. Similarly, the
144 simultaneous administration of the hydro alcoholic extract of STN with CCl_4
145 caused a dose related lowering in the levels of the AST and ALT by 60% and 58%
146 respectively in comparison with the CCl_4- challenged group. Remarkably, the
147 treatment of the rats with the ETN or STN extract alone caused a significant
148 decline in the AST and ALT concentrations as compared to the control group (Fig.
149 2).

150 *2.5. Histopathological examination with hematoxylin and eosin (H and E) stain*

151 Liver sections taken from the control group stained with H&E displayed normal
152 histological structure of the central vein and surrounding hepatocytes with no
153 histopathological alterations (Fig.3A). Treatment with ETN or STN only didn't
154 exhibit any change in the normal liver architecture (Fig.3F& 3I). Exposure to CCl_4
155 triggered a thickening and fibrosis with fat cells deposition in the hepatic capsule
156 associated with extended fibrosis to the hepatic parenchyma between the
157 degenerated hepatocytes, in addition to the portal area that showed also fibrosis
158 which was extended to the parenchyma between the degenerated hepatocytes with
159 inflammatory cells infiltration and congestion in the portal vein (Fig.3B). The rats
160 concurrently treated with silymarin showed restoration of normal histological
161 structure (Fig.3C). Animals co-treated with ETN (100 mg/kg) presented a mild
162 congestion in the central vein (Fig.3D), while ETN lower dose showed portal vein

Peer-reviewed version available at Molecules 2018, 23, 1411; doi:10.3390/molecules23061411

163 congestion with inflammatory cells infiltration in the portal area (Fig. 3E). On the
164 other hand, groups co-administered STN (100 mg/kg) showed only focal
165 infiltration with inflammatory cells (Fig.3G), while STN co-treatment (50 mg/kg)
166 revealed diffuse cell infiltration with hepatocellular degeneration (Fig. 3H).

167 *2.6. Oxidative stress parameters*

168 As shown in (Fig. 4A) the CCl_4 intoxication significantly reduced the GSH level
169 by 50% as compared to the control group. Concomitant treatment with silymarin
170 and CCl_4 offered a significant protection against CCl_4 intoxication by significantly
171 increasing the GSH level reaching 230% as compared to the CCl_4 groups.
172 Furthermore, animals treated with the ETN or STN extract along with CCl_4 showed
173 an increase in the level of GSH by 147% and 328% respectively when compared to
174 group exposed to CCl_4 in a dose related manner. Remarkably, the administration of
175 the ETN or STN alone revealed a significant increment in the level of GSH
176 reaching 214% and 185% in comparison to the control group.

177 Lipid peroxidation measured as malondialdehyde (MDA) concentration showed a
178 significant 3-fold increase as a result of CCl_4 administration, as compared to the
179 control group. The administration of silymarin in tandem with CCl_4 exhibited a
180 significant inhibition in the rise of MDA level and kept it within the normal values
181 when compared to the control. Moreover, animals treated with the ETN or STN
182 extract in addition to CCl_4 showed a dose related reduction in the level of MDA by

Peer-reviewed version available at Molecules 2018, 23, 1411; doi:10.3390/molecules23061411

183 42% and 54% respectively when compared to CCl_4 intoxicated group. On the other
184 hand, there was no significant change in the lipid peroxidation when the animals
185 were administered the ETN or STN extract alone in comparison with the control
186 group (Fig. 4B).
187 Intoxication with CCl_4 brought an evident reduction in the catalase activity by 62%
188 as compared to the control group. Treatment of animals with silymarin
189 concomitantly with CCl_4 triggered significant increased the catalase activity level
190 to reach 248% as compared to the CCl_4-exposed group. Moreover, animals treated
191 by ETN or STN extract along with CCl_4 exhibited a dose related increase in the
192 activity of catalase reaching 200% and 224% respectively when compared to group
193 exposed to CCl_4.. Interestingly The administration of the ETN or STN alone
194 revealed a significant raise in the catalase activity by 88% and 81% after
195 comparison with the control group (Fig. 4C).
196 *2.7. Liver fibrosis markers*
197 Liver fibrosis was assessed biochemically by determining collagen accumulation
198 indices in terms of its main component, hydroxyproline. Measurement of
199 hydroxyproline assured the histological observation of enhanced liver fibrosis by
200 CCl_4. As the liver hydroxyproline content in the CCl_4 challenged group was 513 %
201 as compared to the control group. The animal treatment with silymarin together
202 with CCl_4 significantly lowered the hydroxyproline content in liver by 73% with

Peer-reviewed version available at Molecules 2018, 23, 1411; doi:10.3390/molecules23061411

respect to the CCl_4 exposed group. Moreover, animals treated with the ETN or STN extract in addition to CCl_4 showed a dose related significant reduction in the level of liver hydroxyproline by 64% and 71% respectively when compared to CCl_4 intoxicated group. On the other hand, there was no significant alteration in the hydroxyproline liver content when the animals were administered the ETN or STN extract alone in comparison with the control group (Fig.5).

The immunohistochemical examination of α-SMA expression revealed minimal staining in the blood vessels of the control group (Fig.6A). A marked expression was observed periportally and perisinusoidally in the CCl_4 exposed group as shown by the intense brown staining and optical density (O.D) of 127% with respect to the control group (Fig.6B). Animals co-treated with silymarin, ETN or STN extract markedly attenuated this elevated expression (Fig.6C-E) which was assured by lowering the O.D to 83%, 80% and 77% as compared to the CCl_4 exposed group.

2.8. Inflammatory markers

The measurement of the TNF-α and COX-2 content was carried out using ELISA technique. Exposure to CCl_4 caused a significant rise in the TNF-α value by 133% with respect to the control group. The concurrent treatment with silymarin, ETN or STN suppressed the rise in the TNF-α by 53%, 42.5% and 42% respectively, in comparison with the CCl_4 challenged group (Fig. 7A).

The COX-2 levels showed a similar pattern to that of TNF-α by a 3-fold increase in the COX-2 concentration upon exposure to CCl_4.The effect of the intoxication was ameliorated by co- administration of silymarin, ETN or STN that reduced the COX-2 level to 41%, 43% and 35% respectively, as compared to the group intoxicated with CCl_4 (Fig. 7B).

NF-κB was assessed immunohistochemically by detecting the activated subunit p65 in liver tissues. Control rats showed a minimal immunostaining for NF-κB (Fig. 8A). CCl_4 brought an increase in the p65 content in the liver tissues, which was manifested by the intense brown staining that was proven by the significant increase in OD by 33% (Fig. 8B). However, silymarin significantly lowered the expression of NF-κB as well as the OD by 19% with respect to the CCl_4-challenged group. In addition, Co-treatment of rats with ETN or STN significantly reduced the expression of NF-κB, which was assured by the reduction in the OD by12% and 16% respectively, when compared to CCl_4-intoxicated group (Fig. 8D & 8E).

Peer-reviewed version available at *Molecules* **2018**, *23*, 1411; doi:10.3390/molecules23061411

Discussion

The aim of current study was to explore the metabolites profile of *T.nilotica* soluble alcohol fraction of aqueous extract (ETN and STN), assess *in-vivo* antifibrotic activity and the possible underlying mechanism. HPLC/HRESI/MS/MS profiling of ETN and STN highlighted the presence of various polyphenol derivatives, which played an important role in the antioxidant and antifibrotic activities. Interestingly, sulphated polyphenols represented the main components of STN in comparison to ETN. This finding is due to the fact that, same species growing in different geographical locations is subjected to variations due to their occurrence in contrasting ecological and environmental conditions [22]. Despite the reality that ETN and STN exhibited potential antifibrotic activity; the results displayed a significant GSH elevation in animal groups treated with STN when compared to that treated with ETN or even the control rats. This could be referred to the high content of sulphated polyphenols present in STN, which assure the fact reported earlier that the intake of sulphated polyphenols significantly influence GSH synthesis [23]

Polyphenols are well-known for their antioxidant and anti-inflammatory properties on both *in-vitro* and *in-vivo* experimental models [24]. Accumulating evidence shows that inflammation - in addition to increased oxidative stress - plays an important role in the development of different liver diseases including fibrosis

[25]. According to the current and former study results, *T. nilotica* is reported as a rich source of various polyphenol compounds [26]. In the present study, the ORAC assay results stand in line with the calculated total phenolic content, showing that the radicale scavenging capacity of ETN and STN fractions could be a result of the high phenolic content of both extracts.

Concerning the antifibrotic activity, ETN and STN were investigated against CCl_4-induced fibrosis in rats. In this regard, CCl_4 is considered as one of the most regularly used hepatotoxins in the experimentally-induced liver diseases in animals [27]. Its hepatotoxic effect is initiated by cytochrome P450 2E1 that converts CCl_4 to the highly reactive trichloromethyl radical ($CCl_3^{\bullet}$) which is afterward transformed into more destructive trichloromethyl peroxy radical ($CCl_3OO^{\bullet}$) in the presence of oxygen [28]. The generated free radicals cause injury of hepatocellular membrane via depleted GSH content, increased lipid peroxidation, and release of inflammatory mediators from activated inflammatory cells that in turn potentiate CCl_4-induced hepatic injury [29].

In the present study, CCl_4 caused a significant elevation in serum ALT and AST, indicating hepatocellular inflammation and necrosis [30]. Co- treatment of animals with ETN or STN significantly alleviated such progressive hepatic changes. Silymarin was used as a standard antifibrotic agent due to its well-known hepatoprotective ability [31]. These effects were further proven by

277 histopathological examination of the CCl_4 animals co-treated with the extract or
278 silymarin, which presented minimal hepatic tissues disfiguring as compared to the
279 CCl_4-exposed rats.

280 Lipid peroxidation (measured as MDA) is recognized as one of the principal
281 steps of CCl_4-induced liver injury, as a result, the antioxidant activity is a very
282 important property in a hepatoprotective agents. In fact, MDA has been used for a
283 long time as a biomarker of oxidative stress [32,33]. The increase of MDA reflects
284 enhanced lipid peroxidation and tissue injury. Catalase (a tetrameric heme protein),
285 is one of the major intracellular antioxidant enzymes. Its function is to protect cells
286 from the accumulation of H_2O_2 by catalyzing its decomposition into water and
287 oxygen [34]. The reduced catalase (CAT) activity is a proof for compromised
288 enzymatic protection against tissue damage caused by elevated oxidative stress. In
289 contrast, GSH represents the non-enzymatic part of the host antioxidant defense
290 mechanism. It can effectively scavenge free radicals, while being oxidized by
291 glutathione peroxidase into glutathione disulfide which can be reduced back to
292 GSH by glutathione reductase with the consumption of NADPH [35]. GSH can
293 also react with various electrophiles, physiological metabolites and xenobiotics to
294 form mercapturates, which are catalyzed by other antioxidant enzymes.

295 In this study, there was a marked increase in MDA with concomitant
296 decrease in GSH and CAT activity after chronic CCl_4 challenge. However, ETN

Peer-reviewed version available at Molecules 2018, 23, 1411; doi:10.3390/molecules23061411

297 and STN extracts and standard silymarin kept the MDA levels close to or within
298 the normal values. In another context, ETN, STN and silymarin triggered a
299 significant increase in the CAT activity making it closer to the normal values. As
300 for the GSH content, the silymarin and ETN prevented its consumption, while STN
301 significantly raised the GSH level even above control which could count for the
302 STN efficient antioxidant activity. The observed results are in agreement with
303 earlier studies that showed that several antioxidants possess potential protective
304 effects against CCl_4 induced liver fibrosis [36,37] .

305 Interestingly, NF-κB is a transcriptional regulator of genes involved in
306 immunity, inflammatory response, cell fate, and function [38]. Kupffer cells
307 display powerful NF-κB activation in response to liver injury by CCl_4 and the
308 oxidative damage. This results in production and secretion of proinflammatory
309 cytokines such as TNF-α which is strongly implicated as a fibrosis promoter [39].
310 Accordingly, the persistent elevation in the levels of NF-κB promote the secretion
311 of inflammatory and chemotactic factors in hepatocytes and thereby worsen
312 hepatic inflammation and fibrosis [40] . In this context, several studies showed that
313 downregulation of NF-κB expression and subsequent inflammatory cascade is
314 capable of alleviating CCl_4 induced hepatic fibrogenesis [41,42]. Of the various
315 kinds of inflammatory mediators; TNF-α plays an important role in the
316 pathogenesis of liver fibrosis through activation of Kupffer cells. TNF-α stimulates

317 the release of cytokines from the macrophages and induces phagocyte oxidative
318 metabolism [43]. Thus, a vicious cycle is established in the hepatocytes: TNF-α
319 promotes NF κB activation, and NF-κB leads to enhanced production of additional
320 TNF- α. This cycle eventually alters the structure of the hepatocytes, and impairs
321 their function, consequently, prolonged activation of NF-κB leads to perpetuated
322 inflammatory responses [44]. Moreover, the upregulation of COX-2 has been
323 demonstrated in human liver cirrhosis as a result of active inflammation. [45,46].
324 In the current study, the administration of silymarin, ETN and STN concomitantly
325 with CCl_4 significantly reduced the expression of NF-κB and hence inhibited the
326 downstream inflammatory cascade as evidenced by the significant inhibition of the
327 augmented hepatic levels of TNF-α and COX-2 demonstrating the satisfactory
328 anti-inflammatory properties of the extracts

329 Hydroxyproline is one of the sensitive markers that significantly rises during
330 fibrosis reflecting the increase in the synthesis of collagen [47]. In addition to
331 collagen, expression of the microfilament protein "α-SMA" has been explored as a
332 marker for activation hepatic stellate cells and hence hepatic fibrosis [48]. In this
333 study, there was a significant increase in the hydroxyproline content associated
334 with α-SMA overexpression due to CCl_4 exposure. Co-administration of ETN,
335 STN or silymarin offered a decrease in the hydroxyproline level along with

reduction in the α-SMA expression. It is important to note that all of the effects caused by the co-treatment with ETN or STN were dose dependent.

From the available results, it could be concluded that the ETN and STN presents a significant *in-vivo* dose related antifibrotic activities, which in turn may be due to the polyphenols content. The underlying mechanism could be – at least partly - due to restraining of the oxidative stress through GSH replenishment along with inhibiting the inflammatory response. These findings stands in line with previous reports that confirms the antifibrotic activity of quercetin [49] [50], kaempferol [51], gallic acid [52] or falvonoids [53]. In addition to the earlier report which refer the *in-vivo* hepatoprotective properties of *T. nilotica* flowers to its phenolic constituents [8].

Peer-reviewed version available at Molecules 2018, 23, 1411; doi:10.3390/molecules23061411

3. Materials and methods

3.1. Materials

The aerial parts of *T. nilotica* were collected from the campus of German university, Cairo, Egypt and from Al-Taif Mountain, Saudi Arabia, March, 2015. Both plants were collected at the flowering stage. The authenticity of the species was confirmed by Dr. Mohamed El Gebaly (Professor of Taxonomy at the National Research Center, Egypt). A voucher specimen was deposited at the herbarium of department of pharmacognosy, faculty of pharmacy, Ain Shams University, Egypt. Sample was kept under voucher number PHG-P-TN194. Ellman's reagent [5,5-dithio-bis(2-nitrobenzoic acid); DTNB], reduced glutathione (GSH), bovine serum albumin, chloramine-T, *p*-dimethylaminobenzaldehyde (PDMA), hydroxyproline, and thiobarbituric acid (TBA) were purchased from Sigma-Aldrich Chemical Co. (St Louis, MO, USA). Carbon tetrachloride (CCl_4), *n*-butanol, dipotassium hydrogen phosphate (K_2HPO_4), potassium dihydrogen phosphate (KH_2PO_4) and trichloroacetic acid (TCA) were obtained from Al-Gomhoryyah Chemical Co (Egypt).

Peer-reviewed version available at *Molecules* **2018**, *23*, 1411; doi:10.3390/molecules23061411

3.2. Animals

Animal experiments were conducted in accordance with the ethical guidelines (Ain Shams University, Egypt). Male albino rats (100–150 g) were obtained from Nile Co. for Pharmaceutical and Chemical industries, Egypt. Rats were housed in an air-conditioned atmosphere, at a temperature of 25 °C with alternatively 12 hour light and dark cycles. Animals were acclimatized for 2 weeks before performing the study. They were kept on a standard diet and water *ad libitum*. Standard diet pellets (El Nasr, Egypt) contained not less than 20% protein, 5% fiber, 3.5% fat, 6.5% ash and a vitamin mixture.

3.3. Plant extraction

Tamarix nilotica aerial parts (750 g) from Egypt and Saudi Arabia were exhaustively extracted with distilled water at 25°C with stirring (2 Lx3), individually. Each extract was dried at 40 °C under vacuum followed by alcohol extraction. The alcohol soluble fractions of aqueous extracts were dried under vacuum to yield 40.36 g and 44.71 g, respectively. The alcohol soluble fraction of aqueous extract of Saudi *T.nilotica* (STN) and Egyptian *T.nilotica* (ETN) were subjected to further analysis by HPLC/HRESI/MS/MS.

Peer-reviewed version available at Molecules 2018, 23, 1411; doi:10.3390/molecules23061411

3.4. Phenolic content

The total phenolic content of the extract was assessed through Folin–Ciocalteu method [54]. A volume of 200 µL of crude extract (1 mg/mL) were diluted with distilled water to 3 mL then mixed thoroughly with 0.5 mL of Folin–Ciocalteu reagent for 3 min, followed by the addition of 2 mL of 20% (w/v) anhydrous sodium carbonate. The mixture was allowed to stand for 60 min in the dark, and absorbance was measured at 765 nm. The calculation of the total phenolic content was done using gallic acid as a standard via calibration curve with a straight line equation ($y = 0.0012x + 0.5958$) and regression correlation ($R^2 = 0.9994$). Results (Table 3) are presented in equivalent milligrams of gallic acid per 1.0 g of dried extract. All assays were carried out in triplicates.[55]

3.5. LC–HRESI-MS–MS analysis

The chromatographic analysis was performed on an HPLC Agilent 1200 series instrument, the column was Gemini 3 µm C18 110 Å from Phenomenex with dimensions 100 x 1 mm i.d. , protected with RP C18 100 Å guard column with dimensions (5 mm x 300 µm i.d., 5 µm). The mobile phase components were 2% acetic acid (A) and 90% MeOH, 2% acetic acid (B) at a flow rate of 50µL/min. The mobile phase gradient was: 0-60 min, 5% B; 60-70 min, 50% B; 70-80 min, 90% B; 80-90 min, 5% B. The samples were dissolved in 5% MeOH and 2% acetic

acid with a concentration of 1 mg/mL then filtered using a syringe filter with a pore size 0.2 µm. The sample injection volume was 10 µL. A Fourier transform ion cyclotron resonance (FTICR) mass analyzer was used equipped with an electrospray ionization (ESI) system and controlled by X-calibur® software. Detection was performed in the negative and positive ion modes applying a capillary voltage of 36 V and a temperature of 275 °C. The API source voltage was adjusted to 5 kV, and the desolvation temperature to 275 °C. Nitrogen was used as a nebulizing gas with a flow adjusted to 15 L/min. The analytical run time was 89 min and the full mass scan covered the mass range from 150 to 2000m/z with resolution of 100000 [55]. Quantitation by LC-MS-MS; the absolute area and area percent of each peak was calculated by Xcalibur® software with ICIS peak algorithm then exported to Microsoft Excel® software for preparation of graphs and more analysis of data.

3.6. Oxygen radical absorbance capacity (ORAC assay)

Experiments were performed as previously described in black 96-well plates [56]. In each well of a 96-well plate, 150 µL fluorescein (final concentration: 2.5 nM), 25µL Trolox (final concentrations: 0.78–25 µM) or 25µL tested samples were pipetted in quadruplicate. Plate was allowed to equilibrate at 37 ◦C for 30 min. After this time, fluorescence measurements (Ex. 485 nm, Em. 520 nm) were taken

every 90 s; first to determine the background signal. After three cycles 25µL AAPH (final concentration: 60 mM) were added manually in each well with a multi-channel-pipette. Measurements were taken as quickly as possible since the ROS generator displays immediate activity after addition. Fluorescence measurements were continued for 90 min. Half-life time of fluorescein was determined using MS Excel software.

3.7. In-vivo Experimental design

Animals were classified randomly into nine groups (Ten animals per group) and treated for six weeks as follows; Group 1: Rats were given corn oil three times per week and considered as control animals. Group 2: Rats were given CCl_4 (1mL/kg, 1:1 mixture with corn oil, i.p.), twice weekly to induce liver fibrosis [57]. Group 3: Rats were given CCl_4 (1mL/kg, 1:1 mixture with corn oil, i.p.) twice weekly and silymarin oral suspension (100 mg/kg, suspended in distilled water), three times per week at alternating days with CCl_4 and considered as a positive control. Group 4: Rats were given CCl_4 (1mL/kg, 1:1 mixture with corn oil, i.p.) twice weekly and ETN extract (100 mg/kg, orally, dissolved in distilled water) , three times per week at alternating days with CCl_4. Group 5: Rats were given CCl_4 (1mL/kg, 1:1 mixture with corn oil, i.p.) twice weekly and ETN extract (50 mg/kg, orally, dissolved in distilled water), three times per week at alternating days with CCl_4. Group 6: Rats

were given ETN extract alone (100 mg/kg, orally, dissolved in distilled water) three times per week. Group 7: Rats were given CCl_4 (1mL/kg, 1:1 mixture with corn oil, i.p.) twice weekly and STN extract (100 mg/kg, orally, dissolved in distilled water), three times per week at alternating days with CCl_4. Group 8: Rats were given CCl_4 (1mL/kg, 1:1 mixture with corn oil, i.p.) twice weekly and STN extract (50 mg/kg, orally, dissolved in distilled water), three times per week at alternating days with CCl_4. Group 9: Rats were given STN alone (100 mg/kg, orally, dissolved in distilled water) three times per week.

At the end of the sixth week, the rats were anaesthetized and blood samples were collected from the retro-orbital plexus and allowed to clot. Serum was separated by centrifugation at 1000 rpm for 10 min and used for the assessment of liver functions. Then, rats were sacrificed and liver tissues were dissected, weighed and washed with ice-cold saline. Then livers were then homogenized in ice-cold saline using a homogenizer to obtain 20 % homogenate. Aliquots of the liver homogenate were stored at - 80 °C prior to biochemical analysis. In addition, specimens from the three major lobes of each liver were fixed in 10% formalin saline for histopathological and immunohistochemical investigations.

3.8. Assessment of hepatotoxicity indices

Serum aspartate aminotransferase (AST) and alanine aminotransferase (ALT) were determined according to the procedure previously reported [57].

3.9. Assessment of oxidative stress markers

For evaluating GSH reserves, 0.5 mL of the homogenate was added to a tube with 0.5 ml of 10% TCA. For 15 min, the tubes were shaken moderately and intermittently, then a centrifugation at 3000 rpm for 10 min was done. An aliquot of the formed supernatant (0.2 mL) was added to a tube containing 0.1 mL Ellman's reagent and 1.7 mL phosphate buffer, then the absorbance was read at 412 nm within 5 min [58]. The results were expressed as mmol of GSH/mg protein. Lipid peroxidation was measured by calculating the level of thiobarbituric acid reactive substances (TBARS) measured as malondialdehyde (MDA), as per the method of [59]. The reaction was prepared by addition of 0.5 mL of the homogenate to 1.0 mL 0.6% TBA and 2.5 mL of 20% TCA, and then the mixture was heated in a boiling water bath for 20 min followed by cooling and addition of 4 mL *n*-butanol along with shaking. Separation of the alcohol layer was done by 10 min centrifugation at 2000 rpm for and absorbance was measured at 535 nm. The results were expressed as nmole of MDA/mg protein using 1,1,3,3-tetraethoxypropane used as standard. In addition, CAT activity was assessed using commercially available biochemical kit (Biodiagnostics, Egypt)

3.10. Assessment of liver fibrosis

Liver fibrosis was evaluated using 2 different markers; hydroxyproline and α-SMA. The first one was determined according to previously described method

[60]. The procedure utilized a volume of 0.5 ml of 20% liver homogenate which was kept in 1 mL of 6 M HCl for 8 h at 120 °C. A portion of the digested homogenate (25 µL) is added to 25 µL citrate-acetate buffer then 500 µL of chloramine T solution was added and finally the mixture is kept for 20 min at room temperature. Then, 500 µL Ehrlich's solution was added and the mixture is incubated at 65 °C for 15 min. After cooling for 10 min, the color developed was spectrophotometrically measured at 550 nm. The results were presented as µg/g of wet tissue. In addition, α-SMA expression in formalin-fixed paraffin-embedded rat liver was assessed immunohistochemically using monoclonal antibody (MA1-744, ThermoFisher, UK).

3.11. Assessment of inflammatory markers

The TNF-α and COX-2 levels in liver homogenate was performed using commercial ELISA kit Sigma Aldrich Chemical Co. (St Louis, MO, USA) according to the manufacturer's instructions. The quantities of TNF-α and COX-2 were expressed as ng/mg protein. The Protein was calculated using bovine serum albumin as standard [61]. Furthermore, NF-κBp65 subunit expression was assessed immunohistochemically in formalin-fixed paraffin-embedded rat liver using polyclonal antibody (PA5-16545, ThermoFisher, UK).

3.12. Statistical analysis

Data are presented as mean ± SEM, multiple group comparisons were carried out using one-way analysis of variance (ANOVA) followed by the Tukey-Kramer test for post-hoc analysis. Probability values of $P<0.05$ were considered statistically significant. All statistical analyses were performed using GraphPad InStat software, version 3.05 (GraphPad Software, Inc. La Jolla, CA, USA). Graphs were sketched using GraphPad Prism software, version 5.00 (GraphPad Software, Inc. La Jolla, CA, USA).

Conflict of Interest: None to declare.

References

1. Bataller, R.; Brenner, D.A. Liver fibrosis. *Journal of clinical investigation* **2005**, *115*, 209.
2. Trautwein, C.; Friedman, S.L.; Schuppan, D.; Pinzani, M. Hepatic fibrosis: Concept to treatment. *Journal of hepatology* **2015**, *62*, S15-S24.
3. Benyon, R.; Iredale, J. Is liver fibrosis reversible? *Gut* **2000**, *46*, 443-446.
4. Al-Asmari, A.K.; Al-Elaiwi, A.M.; Athar, M.T.; Tariq, M.; Al Eid, A.; Al-Asmary, S.M. A review of hepatoprotective plants used in saudi traditional medicine. *Evidence-Based Complementary and Alternative Medicine* **2014**, *2014*.
5. Migahid, A.M. Flora of saudi arabia. **1978**.
6. Ghazanfar, S.A. *Handbook of arabian medicinal plants*. CRC press: 1994.
7. Boulos, L. Medicinal plants of north africa. *Medicinal plants of North Africa.* **1983**.
8. AbouZid, S.; Sleem, A. Hepatoprotective and antioxidant activities of tamarix nilotica flowers. *Pharmaceutical biology* **2011**, *49*, 392-395.
9. Abouzid, S.F.; Ali, S.A.; Choudhary, M.I. A new ferulic acid ester and other constituents from tamarix nilotica leaves. *Chemical and Pharmaceutical Bulletin* **2009**, *57*, 740-742.
10. Souleman, A.A.; Barakat, H.H.; Hussein, S.A.; El-Mousallamy, A.M.; Nawwar, M.A. Unique phenolic sulphate conjugates from the flowers of tamarix amplexicaulis. *Natural Product Sciences* **1998**, *4*, 245-252.
11. Tomás-Barberán, F.A.; Iniesta-Sanmartín, E.; Ferreres, F.; Tomas-Lorente, F.; Trowitzsch-Kienastt, W.; Wray, V. Trans-coniferyl alcohol 4-o-sulphate and flavonoid sulphates from some tamarix species. *Phytochemistry* **1990**, *29*, 3050-3051.
12. Song, R.; Xu, L.; Zhang, Z.; Tian, Y.; Xu, F.; Dong, H. Determination of gallic acid in rat plasma by lc-ms-ms. *Chromatographia* **2010**, *71*, 1107-1111.
13. Nawwar, M.; Buddrus, J.; Bauer, H. Dimeric phenolic constituents from the roots of tamarix nilotica. *Phytochemistry* **1982**, *21*, 1755-1758.
14. Nawwar, M.; Souleman, A.; Buddrus, J.; Bauer, H.; Linscheid, M. Polyphenolic constituents of the flowers of tamarix nilotica: The structure of nilocitin, a new digalloylglucose. *Tetrahedron letters* **1984**, *25*, 49-52.
15. Nawwar, M.; Souleman, A.; Buddrus, J.; Linscheid, M. Flavonoids of the flowers of tamarix nilotica. *Phytochemistry* **1984**, *23*, 2347-2349.
16. Umbetova, A.K.; Esirkegenova, S.Z.; Chaudri, I.M.; Omurkamzinova, V.B.; Abilov, Z.A. Flavonoids of plants from the genus tamarix. *Chemistry of Natural Compounds* **2004**, *40*, 297-298.
17. Nawwar, M.; Hussein, S.; Ayoub, N.; Hofmann, K.; Linscheid, M.; Harms, M.; Wende, K.; Lindequist, U. Aphyllin, the first isoferulic acid glycoside and other phenolics from tamarix aphylla flowers. *Die Pharmazie-An International Journal of Pharmaceutical Sciences* **2009**, *64*, 342-347.
18. Chen, Y.; Yu, H.; Wu, H.; Pan, Y.; Wang, K.; Jin, Y.; Zhang, C. Characterization and quantification by lc-ms/ms of the chemical components of the heating products of the flavonoids extract in pollen typhae for transformation rule exploration. *Molecules* **2015**, *20*, 18352-18366.
19. Li, W.; Sun, Y.; Liang, W.; Fitzloff, J.F.; Van Breemen, R.B. Identification of caffeic acid derivatives in actea racemosa (cimicifuga racemosa, black cohosh) by liquid chromatography/tandem mass spectrometry. *Rapid communications in mass spectrometry* **2003**, *17*, 978-982.
20. Park, J.B. Isolation and characterization of n-feruloyltyramine as the p-selectin expression suppressor from garlic (allium sativum). *Journal of agricultural and food chemistry* **2009**, *57*, 8868-8872.

21. Orfali, R.S.; Ebada, S.S.; El-Shafae, A.M.; Al-Taweel, A.M.; Lin, W.H.; Wray, V.; Proksch, P. 3-o-trans-caffeoylisomyricadiol: A new triterpenoid from tamarix nilotica growing in saudi arabia. *Zeitschrift für Naturforschung C* **2009**, *64*, 637-643.
22. Spitaler, R.; Schlorhaufer, P.D.; Ellmerer, E.P.; Merfort, I.; Bortenschlager, S.; Stuppner, H.; Zidorn, C. Altitudinal variation of secondary metabolite profiles in flowering heads of arnica montana cv. Arbo. *Phytochemistry* **2006**, *67*, 409-417.
23. Yan, C.C.; Huxtable, R.J. Effect of taurine and guanidinoethane sulfonate on glutathione metabolism in the rat. In *Taurine 3*, Springer: 1998; pp 33-39.
24. Martins, N.; Barros, L.; Ferreira, I.C. In vivo antioxidant activity of phenolic compounds: Facts and gaps. *Trends in Food Science & Technology* **2016**, *48*, 1-12.
25. Poli, G. Pathogenesis of liver fibrosis: Role of oxidative stress. *Molecular aspects of medicine* **2000**, *21*, 49-98.
26. Abdelgawad, A. Tamarix nilotica (ehrenb) bunge: A review of phytochemistry and pharmacology. *J Microb Biochem Technol* **2017**, *9*, 544-553.
27. Johnston, D.E.; Kroening, C. Mechanism of early carbon tetrachloride toxicity in cultured rat hepatocytes. *Basic & Clinical Pharmacology & Toxicology* **1998**, *83*, 231-239.
28. Goeptar, A.R.; Scheerens, H.; Vermeulen, N.P. Oxygen and xenobiotic reductase activities of cytochrome p450. *Critical reviews in toxicology* **1995**, *25*, 25-65.
29. Recknagel, R.O.; Glende, E.A.; Dolak, J.A.; Waller, R.L. Mechanisms of carbon tetrachloride toxicity. *Pharmacology & therapeutics* **1989**, *43*, 139-154.
30. Bahcecioglu, I.H.; Koca, S.S.; Poyrazoglu, O.K.; Yalniz, M.; Ozercan, I.H.; Ustundag, B.; Sahin, K.; Dagli, A.F.; Isik, A. Hepatoprotective effect of infliximab, an anti-tnf-α agent, on carbon tetrachloride-induced hepatic fibrosis. *Inflammation* **2008**, *31*, 215.
31. Saller, R.; Meier, R.; Brignoli, R. The use of silymarin in the treatment of liver diseases. *Drugs* **2001**, *61*, 2035-2063.
32. Lykkesfeldt, J. Malondialdehyde as biomarker of oxidative damage to lipids caused by smoking. *Clinica Chimica Acta* **2007**, *380*, 50-58.
33. Matés, J.M.; Pérez-Gómez, C.; De Castro, I.N. Antioxidant enzymes and human diseases. *Clinical Biochemistry* **1999**, *32*, 595-603.
34. Dong, Y.; Qu, Y.; Xu, M.; Wang, X.; Lu, L. Catalase ameliorates hepatic fibrosis by inhibition of hepatic stellate cells activation. *Frontiers in bioscience (Landmark edition)* **2014**, *19*, 535-541.
35. Fang, Y.-Z.; Yang, S.; Wu, G. Free radicals, antioxidants, and nutrition. *Nutrition* **2002**, *18*, 872-879.
36. Chang, H.-F.; Lin, Y.-H.; Chu, C.-C.; Wu, S.-J.; Tsai, Y.-H.; Chao, J.C.-J. Protective effects of ginkgo biloba, panax ginseng, and schizandra chinensis extract on liver injury in rats. *The American journal of Chinese medicine* **2007**, *35*, 995-1009.
37. Galicia-Moreno, M.; Rodríguez-Rivera, A.; Reyes-Gordillo, K.; Segovia, J.; Shibayama, M.; Tsutsumi, V.; Vergara, P.; Moreno, M.G.; Muriel, P. N-acetylcysteine prevents carbon tetrachloride-induced liver cirrhosis: Role of liver transforming growth factor-beta and oxidative stress. *European journal of gastroenterology & hepatology* **2009**, *21*, 908-914.
38. Elsharkawy, A.M.; Mann, D.A. Nuclear factor-κb and the hepatic inflammation-fibrosis-cancer axis. *Hepatology* **2007**, *46*, 590-597.
39. Racanelli, V.; Rehermann, B. The liver as an immunological organ hepatology 43. *S54-S62* **2006**.
40. Luedde, T.; Schwabe, R.F. Nf-κb in the liver—linking injury, fibrosis and hepatocellular carcinoma. *Nature Reviews Gastroenterology and Hepatology* **2011**, *8*, 108-118.
41. Dang, S.-S.; Wang, B.-F.; Cheng, Y.-A.; Song, P.; Liu, Z.-G.; Li, Z.-F. Inhibitory effects of saikosaponin-d on ccl4-induced hepatic fibrogenesis in rats. *World journal of gastroenterology: WJG* **2007**, *13*, 557.

42. Tipoe, G.L.; Leung, T.M.; Liong, E.C.; Lau, T.Y.H.; Fung, M.L.; Nanji, A.A. Epigallocatechin-3-gallate (egcg) reduces liver inflammation, oxidative stress and fibrosis in carbon tetrachloride (ccl 4)-induced liver injury in mice. *Toxicology* **2010**, *273*, 45-52.
43. Simeonova, P.P.; Gallucci, R.M.; Hulderman, T.; Wilson, R.; Kommineni, C.; Rao, M.; Luster, M.I. The role of tumor necrosis factor-α in liver toxicity, inflammation, and fibrosis induced by carbon tetrachloride. *Toxicology and applied pharmacology* **2001**, *177*, 112-120.
44. Oakley, F.; Mann, J.; Nailard, S.; Smart, D.E.; Mungalsingh, N.; Constandinou, C.; Ali, S.; Wilson, S.J.; Millward-Sadler, H.; Iredale, J.P. Nuclear factor-κb1 (p50) limits the inflammatory and fibrogenic responses to chronic injury. *The American journal of pathology* **2005**, *166*, 695-708.
45. Mohammed, N.; El-Aleem, S.; El-Hafiz, H.; McMahon, R. Distribution of constitutive (cox-1) and inducible (cox-2) cyclooxygenase in postviral human liver cirrhosis: A possible role for cox-2 in the pathogenesis of liver cirrhosis. *Journal of clinical pathology* **2004**, *57*, 350-354.
46. Cheng, J.; Imanishi, H.; Iijima, H.; Shimomura, S.; Yamamoto, T.; Amuro, Y.; Kubota, A.; Hada, T. Expression of cyclooxygenase 2 and cytosolic phospholipase a 2 in the liver tissue of patients with chronic hepatitis and liver cirrhosis. *Hepatology research* **2002**, *23*, 185-195.
47. Ala-Kokko, L.; Stenbäck, F.; Ryhänen, L. Preventive effect of malotilate on carbon tetrachloride-induced liver damage and collagen accumulation in the rat. *Biochemical Journal* **1987**, *246*, 503-509.
48. Friedman, S.L. Molecular regulation of hepatic fibrosis, an integrated cellular response to tissue injury. *Journal of Biological Chemistry* **2000**, *275*, 2247-2250.
49. Qi, L.; Kang, L.; Zhang, J.; Shi, N.; Zhang, M.; Wu, T. Antifibrotic effects of genistein and quercetin in vitro. *Yao xue xue bao= Acta pharmaceutica Sinica* **2001**, *36*, 648-651.
50. Lee, E.S.; Lee, H.E.; Shin, J.Y.; Yoon, S.; Moon, J.O. The flavonoid quercetin inhibits dimethylnitrosamine-induced liver damage in rats. *Journal of pharmacy and pharmacology* **2003**, *55*, 1169-1174.
51. Zhou, Y.; Zhang, S.; Cheng, D.; Li, H.; Tang, Z.; Xue, J.; Cai, W.; Dong, J.; Zhao, L. Preliminary exploration on anti-fibrosis effect of kaempferol in mice with schistosoma japonicum infection. *European Journal of Inflammation* **2013**, *11*, 161-168.
52. El-Lakkany, N.M.; El-Maadawy, W.H.; el-Din, S.H.S.; Saleh, S.; Safar, M.M.; Ezzat, S.M.; Mohamed, S.H.; Botros, S.S.; Demerdash, Z.; Hammam, O.A. Antifibrotic effects of gallic acid on hepatic stellate cells: In vitro and in vivo mechanistic study. *Journal of Traditional and Complementary Medicine* **2018**.
53. Cheng, Y.; Mai, J.-y.; Wang, M.-f.; Chen, G.-f.; Ping, J. Antifibrotic effect of total flavonoids of astmgali radix on dimethylnitrosamine-induced liver cirrhosis in rats. *Chinese journal of integrative medicine* **2017**, *23*, 48-54.
54. Singleton, V.L.; Orthofer, R.; Lamuela-Raventós, R.M. [14] analysis of total phenols and other oxidation substrates and antioxidants by means of folin-ciocalteu reagent. *Methods in enzymology* **1999**, *299*, 152-178.
55. Sobeh, M.; ElHawary, E.; Peixoto, H.; Labib, R.M.; Handoussa, H.; Swilam, N.; El-Khatib, A.H.; Sharapov, F.; Mohamed, T.; Krstin, S. Identification of phenolic secondary metabolites from schotia brachypetala sond.(fabaceae) and demonstration of their antioxidant activities in caenorhabditis elegans. *PeerJ* **2016**, *4*, e2404.
56. Lucas-Abellán, C.; Mercader-Ros, M.; Zafrilla, M.; Fortea, M.; Gabaldón, J.; Núñez-Delicado, E. Orac-fluorescein assay to determine the oxygen radical absorbance capacity of resveratrol complexed in cyclodextrins. *Journal of agricultural and food chemistry* **2008**, *56*, 2254-2259.
57. Wu, J.; Norton, P.A. Animal models of liver fibrosis. *Scandinavian journal of gastroenterology* **1996**, *31*, 1137-1143.
58. Ellman, G.L. Tissue sulfhydryl groups. *Archives of biochemistry and biophysics* **1959**, *82*, 70-77.

651 59. Uchiyama, M.; Mihara, M. Determination of malonaldehyde precursor in tissues by
652 thiobarbituric acid test. *Analytical biochemistry* **1978**, *86*, 271-278.
653 60. Woessner, J.F. The determination of hydroxyproline in tissue and protein samples containing
654 small proportions of this imino acid. *Archives of biochemistry and biophysics* **1961**, *93*, 440-447.
655 61. Lowry, O.H.; Rosebrough, N.J.; Farr, A.L.; Randall, R.J. Protein measurement with the folin
656 phenol reagent. *Journal of biological chemistry* **1951**, *193*, 265-275.

657

658 **Table 1.** Characterization of metabolites from ETN by HPLC-MS/MS in negative ion mode

#	Rt (Min)	$[M-H]^-$	Error (ppm)	MS/MS fragment	Formula	Identity	References
1	3.9	169.0220	-2.9	125.1086	$C_7H_6O_5$	Gallic acid	[12] [13]
2	4.12	301.0421	1.6	273.0435, 179.0096, 150.9980	$C_{15}H_{10}O_7$	Quercetin	[18] [15]
3	6.59	483.0859	-1.2	331.1573, 313.1711, 169.1114	$C_{20}H_{20}O_{14}$	di-Galloyl-glucose (Nilocitin)	[14]
4	14.72	285.0469	2.8	239.0530, 143.1847	$C_{15}H_{10}O_6$	Kaempferol	[18] [15]
5	28.09	197.0531	-1.5	183.2035, 182.1017, 168.1108, 167.1539	$C_9H_{10}O_5$	Methyl gallate-methyl ether	[14]
6	30.61	259.0356	-0.8	229.0872, 179.0628,	$C_{10}H_{12}O_6S$	Coniferyl alcohol-sulphate	[11]
7	36.82	193.0574	2.6	178.1750, 149.1777, 134.0983	$C_{10}H_{10}O_4$	Ferulic acid isomer	[19] [17]
8	42.4	477.1101	2.1	315.0990, 300.1015	$C_{22}H_{22}O_{12}$	Methyl-quercetin-hexoside (Tamarixetin-3-*O*-hexoside)	[16]
9	43.93	273.0145	0.7	229.0810, 193.1538, 178.0940	$C_{10}H_{10}O_7S$	Ferulic acid-sulphate derivative	[10]
10	53.62	314.1315	-0.32	177.0162, 164.1282, 145.1110	$C_{18}H_{19}NO_4$	*n*-Feruloyltyramine*	[20] [21]
11	57.08	287.0299	1.4	272.1937, 207.1997, 192.1747	$C_{11}H_{12}O_7S$	Methyl ferulate-sulphate	[9]
12	58.3	461.0806	-1.7	285.1083, 257.3536	$C_{21}H_{18}O_{12}$	Kaempferol-glucuronide	[15]
13	67.53	315.0587	-1.3	300.1302, 193.1954	$C_{16}H_{12}O_7$	Methyl-quercetin (Tamarixetin)	[16] [9] [17]
14	71.19	299.0624	3	284.1601, 271.2777	$C_{16}H_{12}O_6$	Methyl-kaempferol (Kaempferide)	[9]
15	74.7	395.0154	-0.8	315.1095, 300.2426, 217.0871	$C_{16}H_{12}O_{10}S$	Methyl-quercetin-sulphate (Tamarixetin-3-*O*-sulphate)	[11] [17]
16	75.12	379.0195	1.8	299.1220, 284.2777	$C_{16}H_{12}O_9S$	Kaempferol-methyl ether -sulphate	[11]
17	75.89	393.0366	-2	313.1219, 298.0152, 283.8303	$C_{17}H_{14}O_9S$	Kaempferol-dimethyl ether -sulphate	[15]

659

660 * detected only through inspection of the positive ion mode. ETN is the alcohol soluble fraction of aqueous extract
661 of *T.nilotica* from Egypt

662

663 **Table 2.** Characterization of metabolites from STN by HPLC-MS/MS in negative ion mode

#	Rt (Min)	$[M-H]^-$	Error (ppm)	MS/MS fragment	Formula	Identity	References
1	4.81	169.0213	1.18	125.1079	$C_7H_6O_5$	Gallic acid	[12] [13]
2	5.26	301.0425	0.33	273.0441, 179.0084,150.9916	$C_{15}H_{10}O_7$	Quercetin	[18] [15]
3	6.47	483.0851	0.41	331.1561, 313.1709, 169.1116	$C_{20}H_{20}O_{14}$	di-Galloyl-glucose (Nilocitin)	[14]
4	10.57	285.0483	-2.10	239.0536, 143.1841	$C_{15}H_{10}O_6$	Kaempferol	[18] [15]
5	23.52	197.0533	-2.52	183.2027, 182.1022, 168.1119, 167.1531	$C_9H_{10}O_5$	Methyl gallate--methyl ether	[14]
6	25.62	259.0351	1.15	229.0876, 179.0632	$C_{10}H_{12}O_6S$	Coniferyl alcohol-sulphate	[11]
7	37.82	273.0151	-1.46	229.0806, 193.1527, 178.0947	$C_{10}H_{10}O_7S$	ferulic acid-sulphate derivative	[10]
8	53.72	314.1319	-1.60	177.0161, 164.12874, 145.1103	$C_{18}H_{19}NO_4$	*n*-Feruloyltyramine*	[20] [21]
9	56.93	287.0301	0.69	272.1925, 207.2002, 192.1733	$C_{11}H_{12}O_7S$	Methyl ferulate-sulphate	[9]
10	57.16	461.0795	0.65	285.1096, 257.3548	$C_{21}H_{18}O_{12}$	Kaempferol-glucruonide	[15]
11	68.48	315.0589	-1.90	300.1311, 193.1967	$C_{16}H_{12}O_7$	Methyl-quercetin (Tamarixetin)	[16] [9] [17]
12	71.17	299.0629	1.33	284.1607, 271.2769	$C_{16}H_{12}O_6$	Methyl-kaempferol (Kaempferide)	[9]
13	72.56	395.0159	-2.02	315.1085, 300.2417, 217.0865	$C_{16}H_{12}O_{10}S$	Methyl-quercetin-sulphate (Tamarixetin-sulphate)	[11] [17]
14	74.06	379.0191	2.89	299.1221, 284.2782	$C_{16}H_{12}O_9S$	Kaempferol-methyl ether-sulphate	[11]
15	75.60	393.0368	-2.54	313.1212, 298.0147, 283.8312	$C_{17}H_{14}O_9S$	Kaempferol-dimethyl ether-sulphate	[15]

664

665 * detected only through inspection of the positive ion mode. STN is the alcohol soluble fraction of aqueous extract
666 of *T.nilotica* from Saudi Arabia

667 **Table 3.** Total phenolic content of ETN and STN

	Total phenolic content (mg GA/ gm dry extract)
ETN	95.1
STN	111.8

668

669

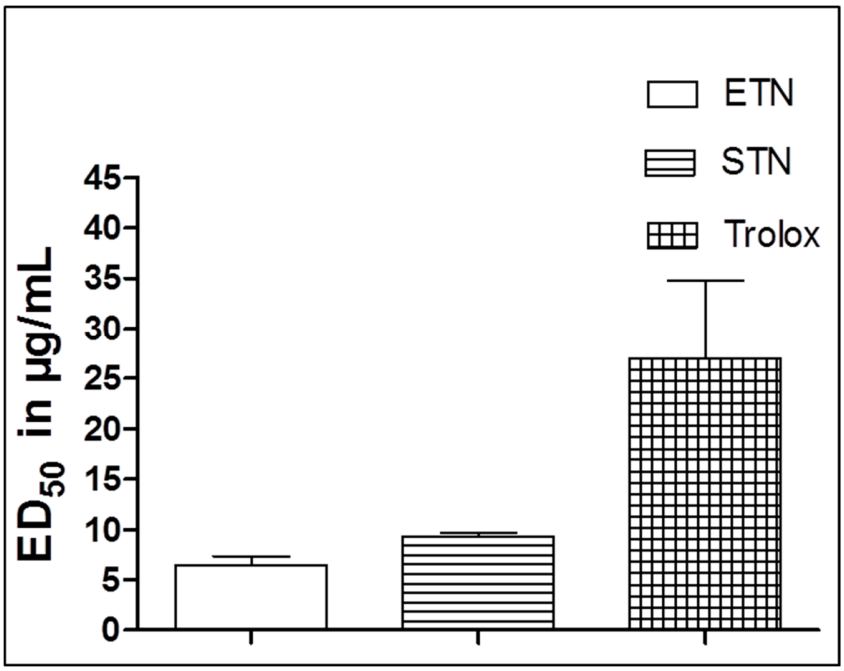

Fig.1.: Radicle scavenging activity of ETN and STN.
Results are given as mean values ± SD of n=3

676

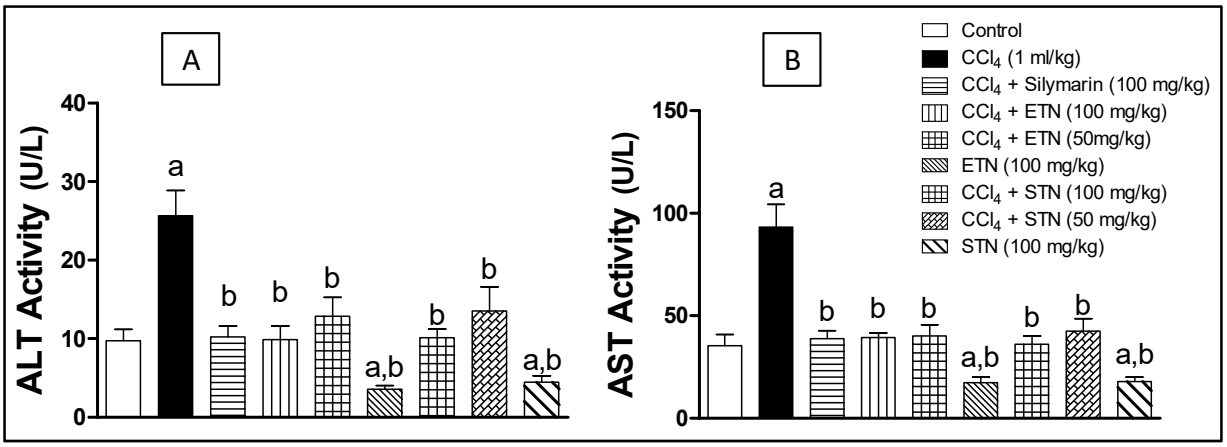

677

678 **Fig. 2.** Effect of ETN and STN on ALT (Panel A) and AST (Panel B) serum activities in rats
679 subjected to chronic CCl_4 intoxication.

680 * Data are the mean ± SD (n=10).

681 a or b: Significantly different from control or CCl_4 group respectively at $p < 0.05$ using ANOVA
682 followed by Tukey-Kramer as a post-hoc test.

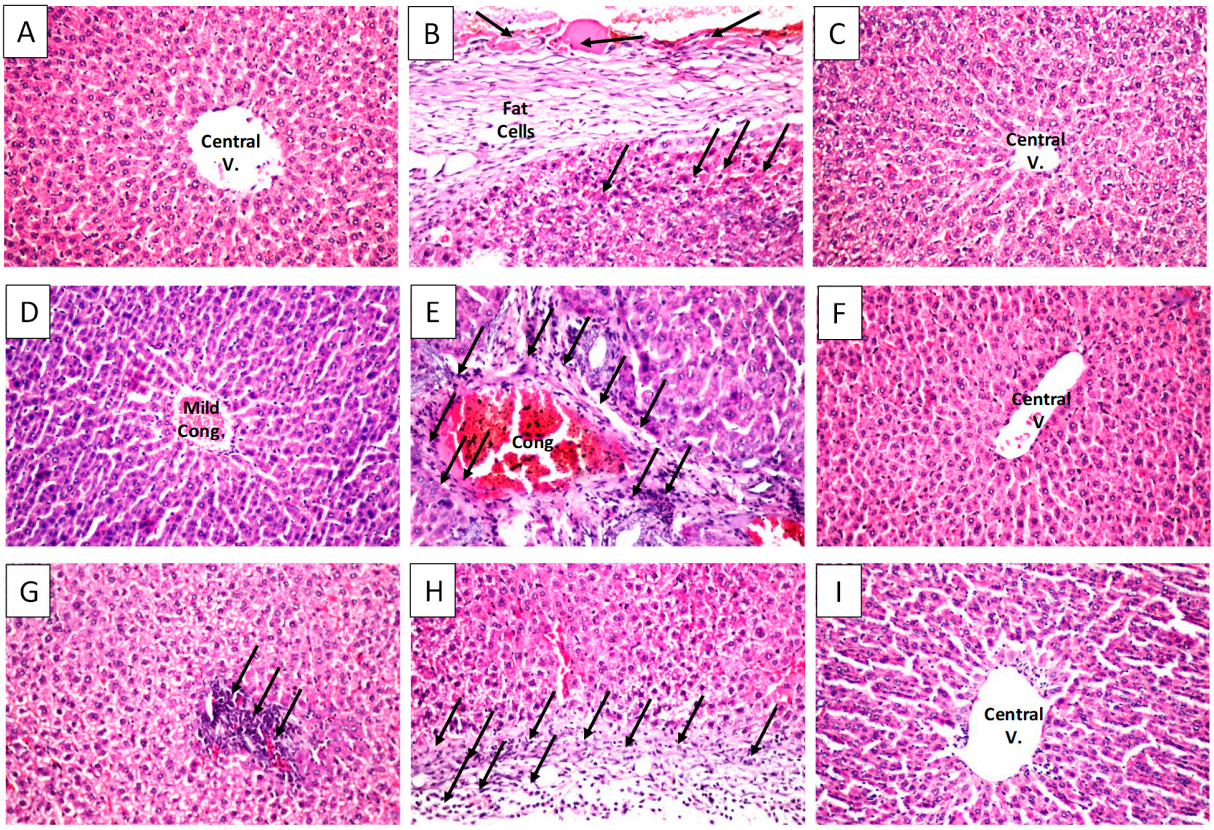

Fig. 3. Representative photomicrographs of liver sections stained with H and E (100x).

A: section taken from a control rat liver showing normal central vein and hepatic architecture. **B**: section taken from rat liver exposed to CCl_4 showing thickening and fibrosis with fat cells deposition in the hepatic capsule associated with extended fibrosis to the hepatic parenchyma between the degenerated hepatocytes (arrows). **C**: section taken from rat liver exposed to CCl_4 and treated with silymarin (100 mg/kg) showing restoration of normal histological structure. **D**: section taken from rat liver exposed to CCl_4 and treated with ETN (100 mg/Kg) showing mild congestion in the central vein. **E**: section taken from rat liver exposed to CCl_4 and treated with ETN (50 mg/Kg) showing portal vein congestion with inflammatory cells infiltration in the portal area. **F**: section taken from rat liver exposed only to ETN (100 mg/Kg) showing no histopathological alterations. G: section taken from rat liver exposed to CCl_4 and treated with STN (100 mg/Kg) showing focal inflammatory cells infiltration (arrows). **H**: section taken from rat liver exposed to CCl_4 and treated with STN (50 mg/Kg) showing diffuse inflammatory cells infiltration (arrows), with hepatocytes degeneration. **I**: section taken from rat liver exposed only to STN (100 mg/Kg) showing normal liver architecture.

Preprints (www.preprints.org) | NOT PEER-REVIEWED | Posted: 11 May 2018 doi:10.20944/preprints201805.0175.v1

Peer-reviewed version available at Molecules 2018, 23, 1411; doi:10.3390/molecules23061411

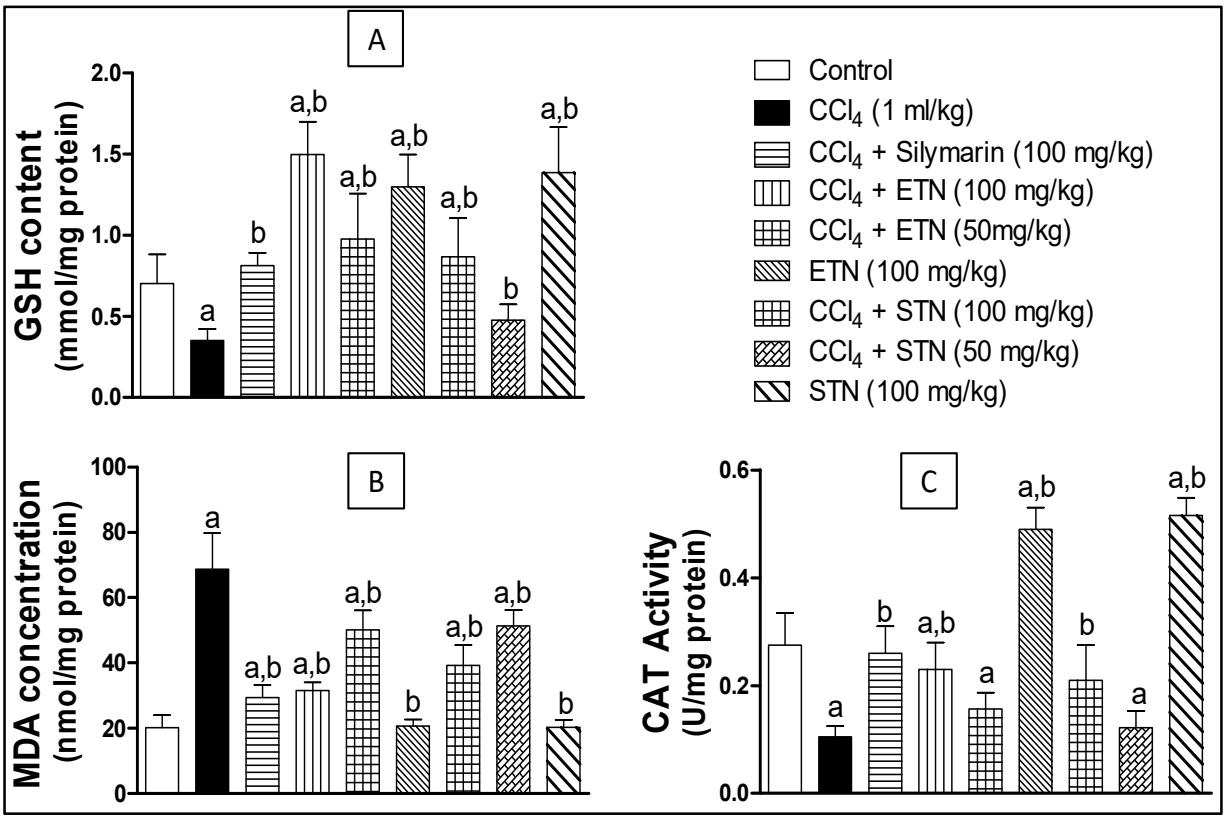

699

700 **Fig. 4. .** Effect of ETN and STN on hepatic GSH content (Panel A), lipid peroxidation as MDA
701 concentration (Panel B), Catalase enzymatic activity (Panel C) in rats subjected to chronic CCl_4
702 intoxication.

703 * Data are the mean ± SD (n=10).

704 a or b: Significantly different from control or CCl_4 group respectively at $p < 0.05$ using ANOVA
705 followed by Tukey-Kramer as a post-hoc test.

706

707

708

709

710

711

712

713

714

715

716

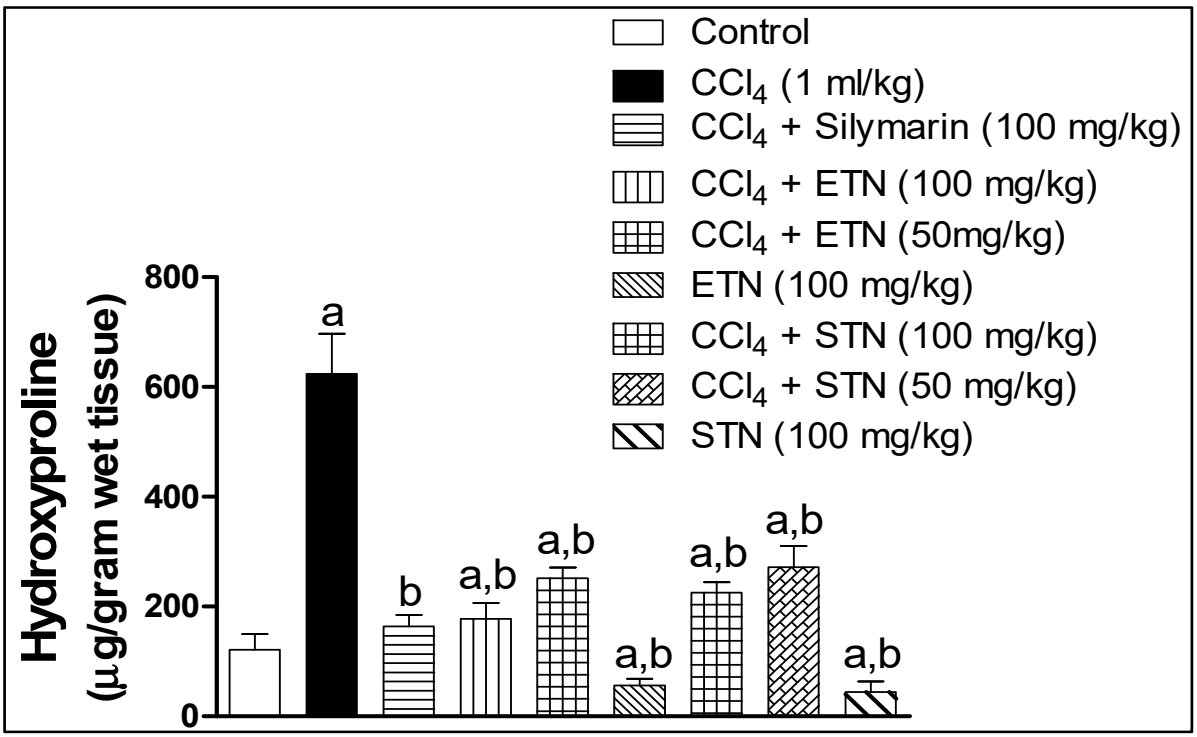

717 **Fig. 5.** Effect of ETN and STN on liver hydroxyproline content rats subjected to chronic CCl_4
718 intoxication.

719 * Data are the mean ± SD (n=6).

720 a or b: Significantly different from control or CCl_4 group respectively at $P < 0.05$ using ANOVA
721 followed by Tukey-Kramer as a post-hoc test.

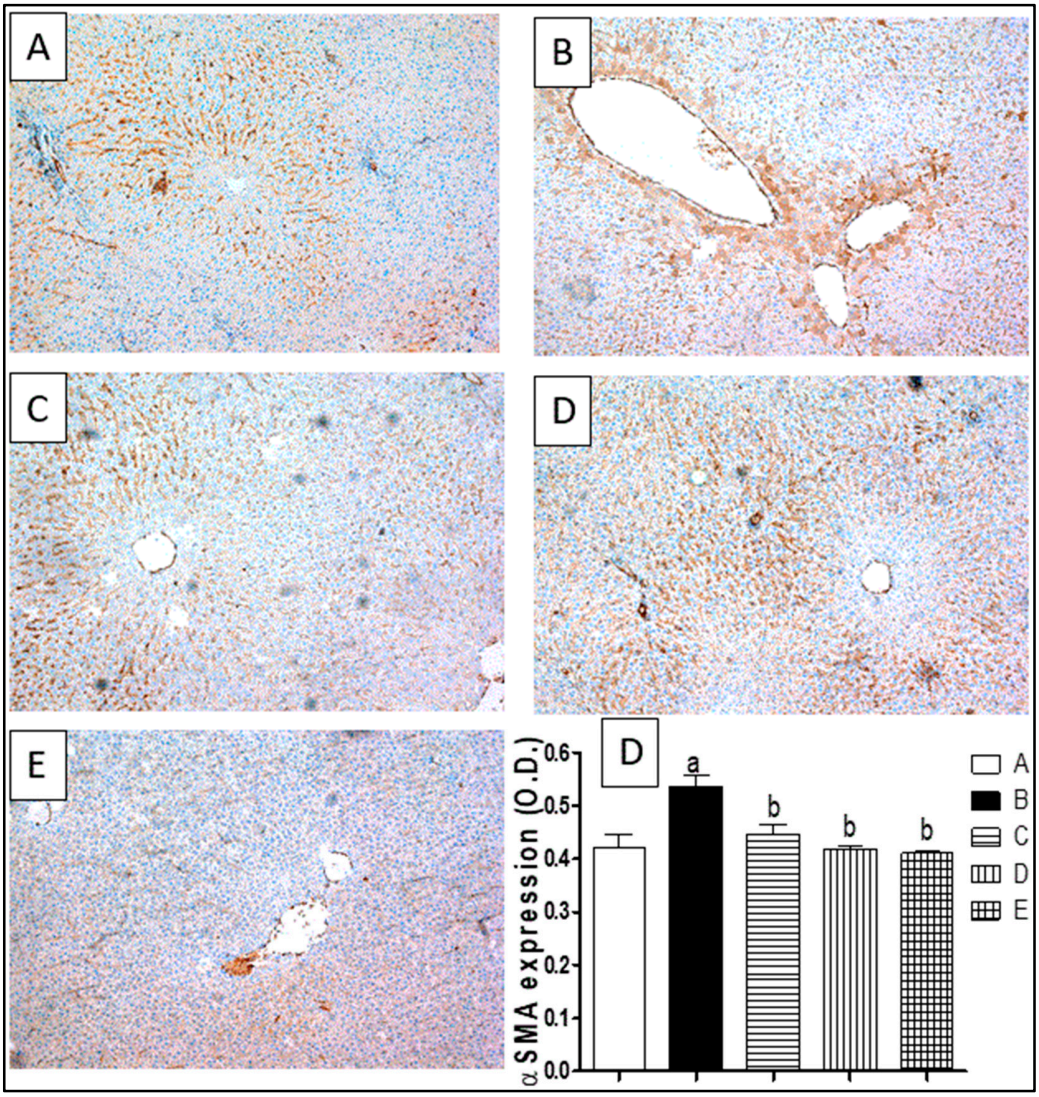

Fig. 6. Expression of alpha smooth muscle actin (α-SMA) by immunohistochemical staining (×100).

A: Photomicrograph of liver section of control rats showing minimal immunostaining for *α*-SMA. B: Photomicrograph of liver section of CCl_4 intoxicated rats showing extensive *α*-SMA expression of as shown by the intense brown staining. C: Photomicrograph of liver section of (CCl_4 / Silymarin) treated rats showing limited *α*-SMA expression. D: Photomicrograph of liver section of rats concurrently treated with CCl_4 (1ml/kg) twice a week and ETN (100 mg/kg) three times per week, showing limited *α*-SMA expression. E: Photomicrograph of liver section of rats simultaneously treated with CCl_4 (1ml/kg) twice a week and STN (100 mg/Kg) three times per week, showing minimal *α*-SMA expression. F: A graphical representation of the *α*-SMA expression as optical density (O.D) for the liver sections from different groups, where a or b express the significant difference from control or CCl_4 group respectively at $P < 0.05$ using ANOVA followed by Tukey-Kramer as a post-hoc test.

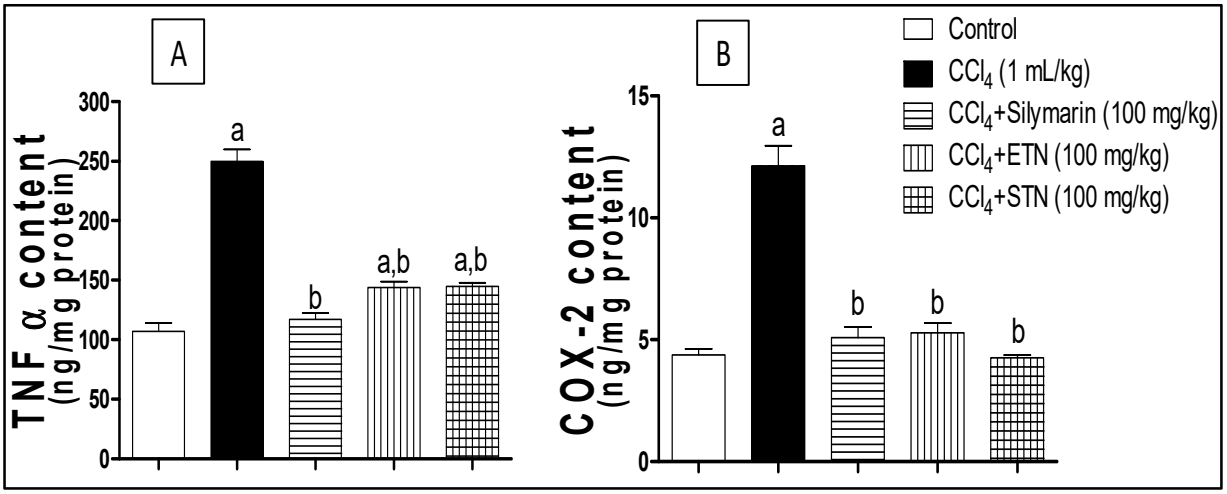

Fig. 7. Effect of ETN and STN aqueous alcohol extracts on hepatic TNF-α (Panel A) and COX-2 content (Panel B) in rats subjected to chronic CCl_4 intoxication.

* Data are the mean ± SD (n=6).

a or b: Significantly different from control or CCl_4 group respectively at $p < 0.05$ using ANOVA followed by Tukey-Kramer as a post-hoc test.

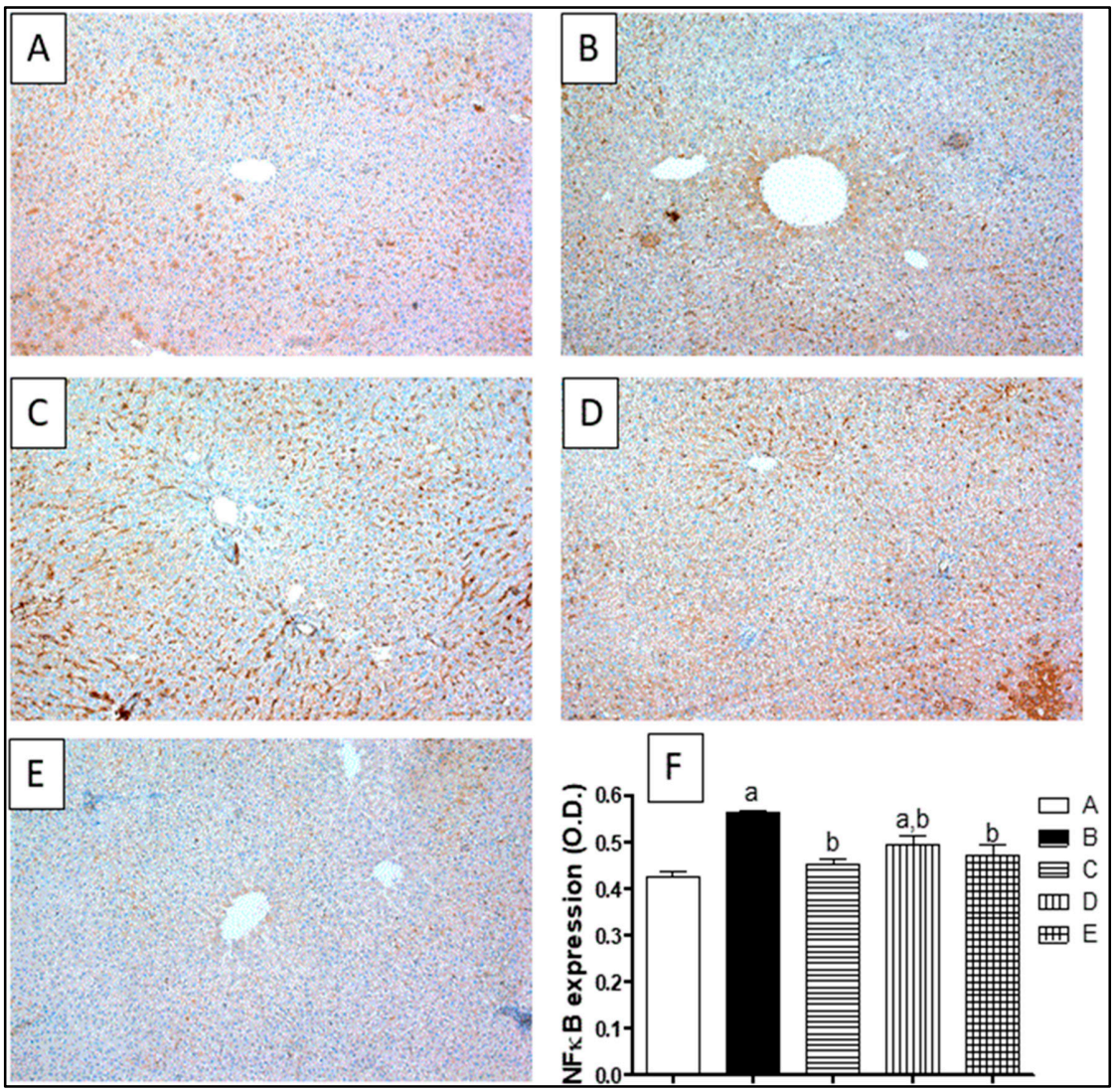

Fig. 8. Expression of Nuclear Factor kappa B (NF-κB) by immunohistochemical staining (100X).

A) Photomicrograph of liver section of control rats showing minimal immunostaining for NF-κB. **B)** Photomicrograph of liver section of CCl_4 intoxicated rats showing increased NF-κB expression of as shown by the intense brown staining. **C)** Photomicrograph of liver section of (CCl4 / Silymarin) treated rats showing limited NF-κB expression. **D)** Photomicrograph of liver section of rats concurrently treated with CCl_4 (1ml/Kg) twice a week and ETN (100 mg/Kg) three times per week, showing limited NF-κB expression. **E)** Photomicrograph of liver section of rats simultaneously treated with CCl_4 (1ml/Kg) twice a week and STN (100 mg/Kg) three times per week, showing decreased NF-κB expression. **F)** A graphical representation of the NF-κB expression as optical density (O.D) for the liver sections from different groups, where a or b express the significant difference from control or CCl_4 group respectively at $P < 0.05$ using ONE-WAY ANOVA followed by Tukey-Kramer as a post-hoc test